Ninth International Conference on Fast Sea Transportation
FAST2007, Shanghai, China, September 2007

Development of a Nonlinear Simulation for Testing of Control Systems in a General Class of Lifting Body Vessels, SWATHs, and Hydrofoils

Benjamin Rosenthal

Navatek, Ltd., Honolulu, Hawaii, USA

ABSTRACT

The demand for faster, more efficient ships has increased the use of non-traditional technologies such as hydrofoils, lifting bodies, and alternative hull forms, many of which use control systems for improved seakeeping and in some cases to ensure dynamic stability. High-fidelity time-domain methods available to simulate the motion of a ship in a seaway in support of control system design are often computationally expensive, so testing changes in control system parameters can be time consuming; obtaining statistically meaningful data sets can also be computationally prohibitive. Frequency-domain based codes allow the user to design control systems based on an assumed input wave spectrum, but they are very low fidelity and do not permit visualizing the time history of the ship and its actuators. A fast, medium-fidelity simulation would be extremely useful in control system design and testing. Such a simulation must be adaptable to varied ship configurations and compatible with all the non-traditional ships of interest. This paper presents such a simulation as developed for a general class of lifting body/foil borne ships, SWATHS, and mutlihulls; examines the methodology used as well as the assumptions made in development of this simulation; and presents an example of the simulation's results.

Keywords

Nonlinear simulation, control systems, lifting bodies.

1 INTRODUCTION AND OVERVIEW

As the demand for faster, more efficient ships has increased, so has the use of non-traditional technologies such as hydrofoils, lifting bodies, and alternative hull forms in such ships. Many of these ships use control systems for improved seakeeping, and in some cases, to ensure dynamic stability.

Currently several extremely accurate time-domain free surface codes exist that can reliably model the motion of a ship in a seaway (Beck & Reed 2000) and that are capable of accurately modeling lifting bodies and hydrofoils. However, these codes are typically limited in the types of hull forms they are capable of analyzing and so non-traditional ships may not run successfully. Additionally, since they are not set up for ship control system testing, there is no way for a user who designs a control system to test its effectiveness using the current time-domain seakeeping codes. Even if this were possible, the computational cost of these codes is extremely high and therefore any slight modifications to control system parameters would lead to extremely long waits before the results can be examined.

There are also several commercial and developmental frequency-domain seakeeping codes available (Beck & Reed 2000). These programs have the advantage of being extremely fast in producing results; however, their accuracy is typically much lower than that of the time-domain seakeeping codes, it is not possible to visualize the results, and analysis is limited to the linear regime. The control system and the actuation system must also be transformed to the frequency domain before they can be analyzed.

In response to the limitations noted above, a nonlinear simulation was developed for use in the analysis of a general class of lifting body supported/foil supported ships and boats. In general, the simulation takes any number of hulls separately or in combination with any number of arbitrarily-shaped lifting bodies or hydrofoils. Fully submerged hulls are also included such as SWATHs.

The goal in generating this simulation was to produce a medium-fidelity code that could easily adapt to any hull form and give a reasonably accurate answer in as short a period of time as possible. The solution had to be accurate enough to give the user confidence in the design of a control system, and the results had to be generated in a short enough period of time that the user could easily check the effects of any modifications to control system parameters.

For ease of code development, the simulation was created using MATLAB. Because of its extensive library of intrinsic functions, the MATLAB environment is very convenient for developing time-domain simulations and control system designs. The simulation was designed to be as user-friendly as possible within reasonable programming allowances. For this reason, all geometry is entered using the IGES format, which allows the user to run simulations using files generated directly from their usual CAD environment. All other required input information is entered as ASCII text.

The first section of the simulation estimates the forces generated by the hull(s). A simple planing model is included as well as a nonlinear buoyancy model based on the instantaneous hull position. Also included for case-specific analyses is an aerodynamic model. Next, the lifting body/hydrofoil dynamics are examined. The forces are computed from a combination of empirical equations and user-supplied information.

The simulation has a representation of a seaway based on a Pierson-Moskowitz spectrum. The seaway model allows for a distributed wave pattern.

The control system is included as a standalone section. This allows new control code of drastically different format to be easily substituted in the simulation. Also included in the control system section is a high-fidelity model of the electronics and actuation systems for our specific control system hardware.

The simulation results are output in several ways. The data is output in tabular form as an Excel spreadsheet, and it is also stored as a MATLAB data file. The information can also be stored as an AVI file allowing the user to visualize the motion of the ship as well as all of its control effectors.

Time integration of the equations of motion is performed using one of four user-selected integrators: Runge-Kutta 4^{th} order; Euler 2^{nd} order; ODE45 (adaptive time stepping) canned routine from MATLAB; and ODE23 (adaptive time stepping) canned routine from MATLAB. If either of the two non-adaptive time stepping routines is chosen, temporal convergence must be examined separately and an appropriate time step length chosen.

2 DETAILED DESCRIPTION OF SIMULATION

2.1 Input Format

The input format for the hull and lifting body section of the simulation is IGES, which was chosen because most CAD environments output IGES files allowing for ease of file transfer. The surfaces imported from the IGES file are than broken into a series of stations with linear elements connecting the points (Piegl & Tiller 1997). The density of the paneling is user-selected, and convergence studies must be examined to ensure sufficient panel density. It should be noted that no error checking is performed as to panel density or normal direction. Therefore, if the user is careless, the solution will be meaningless. Figure 1 presents a graphic representation of a sample boat input including its lifting body and hydrofoils. The hull surfaces and forward lifting body were loaded as IGES files; the flat plate foils, struts, and fins were generated internally based on the user's ASCII inputs.

The IGES representations of the hull and its lifting surfaces are only used for some of the force generation. The hull IGES model is used for the buoyancy calculation and for calculation of surface angles for the planing and aerodynamic forces; the lifting body IGES model is used for computation of buoyancy only.

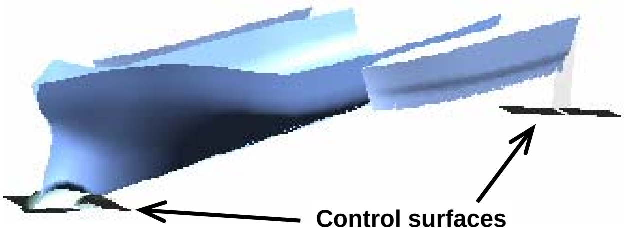

Figure 1: Example of Simulation Input

All other lifting body forces are computed using force coefficients and other necessary values as input by the user. The hydrodynamic force coefficients are usually obtained from a computational fluid dynamics (CFD) analysis, most typically RANS-based (Reynolds-averaged Navier-Stokes). The coefficients can either be compiled in a table or curve/surface fits can be generated and the forces can be represented as equations. Either way, these are entered as ASCII text in a general input file. The other required lifting body parameters are:

- Chord,
- Span,
- Location of center of lift,
- Strut dimensions if connected by a strut,
- Center of location if the body rotates,
- Flap dimensions if flaps are present.

The actuation parameters must also be input. Again, these are entered as ASCII in a general input file. These coefficients encompass:

- Control computer coefficients: filter constants; time constants; update rates.
- Actuator coefficients: hydraulic cylinder properties; solenoid properties.

Upon entry of all necessary inputs, they are compiled in a MATLAB data file and saved to disk. If this data file is present at the start of a simulation, the data is automatically loaded from this file rather than from the user-supplied ASCII data.

2.2 Hull Dynamics

In general, any number of hulls can be examined in the simulation. Because all calculations are for a generalized shape, the simulation simply loops over the number of hulls specified. For this paper, a single hull is assumed with the understanding that multiple hulls are a trivial addition.

Computation of the forces on the hull is separated into four parts: nonlinear buoyancy, nonlinear planing lift, resistance, and aerodynamic effects. Buoyancy is computed at each time step, given the instantaneous hull position and wave pattern. It is assumed that the water surface forms a straight line from the intersection point on one side of the hull to the intersection on the other side of the hull. The sectional area is then computed for each station along the length of the hull, and the displaced volume is computed using trapezoidal integration for all of the stations. Figure 2 shows how the volume of displacement is computed for a nominal hull.

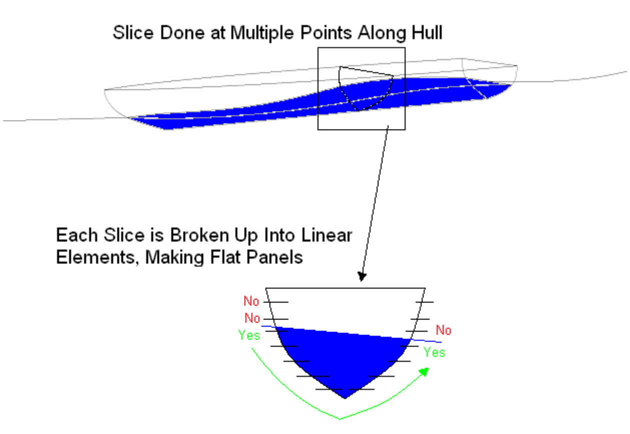

Figure 2: Volume Computation of Nominal Hull

To compute the wetness of a given linear element, the upper and lower ends of the linear element are examined. If both end points of the element are wet, the entire element is assumed wet. If either end point is found to be dry, the distance from the dry point to the free surface is computed and assumed to be the waterline. The waterline is assumed linear between computed points. A binary search routine (Press et al. 1988) is used starting on the port side of the hull and proceeding counterclockwise (as viewed from the stern) to the starboard side. Once the first wet point is found, no further computations are made until a dry point is found on the other side. Once that dry point is found, the search is ended. This simple marching routine allows for decreased computational expense over examining each point. The buoyancy calculation is considered to be nonlinear because the instantaneous waterline is used for every calculation.

If the Froude number of the boat is greater than 1.2, the boat is considered to be planing. In this case, we use Breslin's equations for the planing forces of a chines-dry hull (Breslin 2001), given collectively here as equation (1) to equation (4).

$$R = \tfrac{1}{2}\rho U^2 \tag{1}$$

$$A_b(x) = \frac{1}{\sqrt{\pi}} \frac{\Gamma\left(0.5 + \frac{\beta}{\pi}\right)}{\Gamma\left(1.0 + \frac{\beta}{\pi}\right)} \tag{2}$$

$$C_{L_{2b}} = \frac{\pi^3}{8}\left(\frac{1}{2} - \frac{\beta}{\pi}\right) A_b^2 \tan^3(\alpha)\cot^2(\beta) \tag{3}$$

$$F_z = C_{L_{2b}} R B^2 \tag{4}$$

In these equations, R is the dynamic pressure, ρ is the density of water, U is the free stream velocity, A_b^2 is an empirical formula for the planing area, β is the deadrise, $C_{L_{2b}}$ is the lift coefficient, B is the beam, α is the angle of attack and F_z is the vertical force in dimensional units.

Since the flow at each station is different due to the existence of a seaway, using a single deadrise angle, a single angle of attack, and a single beam, is not appropriate. Therefore, at each station the approach angle, deadrise, and beam are recalculated and a force per unit length is computed. The total planing force is then assumed to be the integration of the force per unit length over all of the wetted stations. The new computation of the planing force is represented in the following equation.

$$R = \tfrac{1}{2}\rho\left(V_x^2 + V_y^2 + V_z^2\right)^2 \tag{5}$$

From equation (5) we see that the dynamic pressure is dependant on the total incoming velocity, allowing for vertical and sideways motion.

$$A_b(x) = \frac{1}{\sqrt{\pi}} \frac{\Gamma\left(0.5 + \frac{\beta(x)}{\pi}\right)}{\Gamma\left(1.0 + \frac{\beta(x)}{\pi}\right)} \tag{6}$$

Here the deadrise and, consequently, the reference area are dependant on the longitudinal location.

Similarly, the angle of attack is dependant on the hull orientation and flow direction at the given longitudinal location leading to a lift coefficient that varies in x as shown in equation (7).

$$C_{L_{2b}} = \frac{\pi^3}{8}\left(\frac{1}{2} - \frac{\beta(x)}{\pi}\right) A_b^2 \tan^3\left(\alpha(x)\right)\cot^2\left(\beta(x)\right) \tag{7}$$

We define a new variable as the distance of the point of examination from the point where the bow of the boat intersects the free surface.

$$L_{wet}(x) = x - x_0 \tag{8}$$

Using equations (5) to (8) we derive an expression for the force per unit length, $f_z(x)$, which can then be evaluated at points along the hull.

$$f_z(x) = \frac{C_{L_{2b}}(x) R B^2(x)}{L_{wet}(x)} \tag{9}$$

Integrating equation (9) leads to the total force in the vertical direction due to planing, F_z.

$$F_z = \int_{x_0}^{x_{max}} f_z(x)\,dx \tag{10}$$

If the boat is planing, the resistance of the boat is computed using Breslin's equations (Breslin 2001), shown here as equations (11) to (15).

$$C_f = \frac{0.075}{\left[\log_{10}\left(R_n\right)-2\right]^2} \tag{11}$$

$$\mu = \frac{1}{2} - \frac{\beta}{\pi} \tag{12}$$

$$\nu = \frac{1}{2} + \frac{\beta}{\pi} \tag{13}$$

$$\frac{\bar{U}}{U} = 1 - \frac{\sqrt{\pi}\mu\Gamma\left(\nu\right)\tan^2\left(\alpha\right)}{2\Gamma\left(\frac{1}{2}+\nu\right)\tan\left(\beta\right)} \tag{14}$$

$$F_X = F_Z \left\{ \tan\left(\alpha\right) + \right. \\ \left. + C_f \frac{\Gamma\left(\frac{1}{2}+\nu\right)}{\pi^{3/2}\mu\Gamma\left(\nu\right)\tan^2\left(\alpha\right)} \frac{\bar{U}^2}{U^2} \sec\left(\beta\right)\tan\left(\beta\right) \right\} \tag{15}$$

In these equations, C_f is the friction coefficient as computed using the ITTC 1957 line, R_n is the Reynolds number, β is again the deadrise, and α is again the angle of attack. The mean velocity along the hull bottom is $\bar{U}$ and U is the free stream velocity.

If we again examine this at each station we see that the resistance force can be computed in much the same manner as the vertical force.

$$C_f = \frac{0.075}{\left[\log_{10}\left(R_n\right)-2\right]^2} \tag{16}$$

$$\mu(x) = \frac{1}{2} - \frac{\beta(x)}{\pi} \tag{17}$$

$$\nu(x) = \frac{1}{2} + \frac{\beta(x)}{\pi} \tag{18}$$

Here we see the two constants from equation (12) and equation (13) are dependant on the longitudinal location in *x*. Rewriting equation (14) and introducing the variable $\Psi\left(x\right)$ leads to equations (19) and (20).

$$\frac{\bar{U}\left(x\right)}{U} = 1 - \frac{\sqrt{\pi}\mu\left(x\right)\Gamma\left(\nu\left(x\right)\right)\tan^2\left(\alpha\left(x\right)\right)}{2\Gamma\left(\frac{1}{2}+\nu\left(x\right)\right)\tan\left(\beta\left(x\right)\right)} \tag{19}$$

$$\Psi\left(x\right) = \frac{\Gamma\left(\frac{1}{2}+\nu(x)\right)}{\pi^{3/2}\mu\left(x\right)\Gamma\left(\nu(x)\right)\tan^2\left(\alpha(x)\right)} \tag{20}$$

Similarly, the angle of attack is now dependant on *x*. The force per unit length is given by equation (21).

$$f_X\left(x\right) = -f_Z\left(x\right) \left\{ \tan\left(\alpha(x)\right) + \right. \\ \left. + C_f \Psi\left(x\right) \frac{\bar{U}\left(x\right)}{U} \sec\left(\beta(x)\right)\tan\left(\beta(x)\right) \right\} \tag{21}$$

Now, as in the lift case, we end up with a resistance force for a longitudinal slice of the hull. Therefore, integrating in *x* gives us the resulting total resistance as shown in equation (22).

$$F_x = \int_{x_0}^{x_{\max}} f_x dx \tag{22}$$

It is clear that the equations for planing lift force and resistance are nonlinear. The use of instantaneous hull parameters and water flow conditions leads to the nonlinearity. A linear assumption is then made, however, that the force for the current station can be found by dividing the total force by the length used in computing that force. Although this is a linear assumption, the resulting approximate force is better than assuming the entire wetted hull is uniform.

If the Froude number is less than 1.1, the boat is considered to be in displacement mode. In this case, no additional vertical force is included. The resistance is computed using the ITTC 1957 line for frictional resistance (Lewis ed. 1988), C_f in equation (11) and equation (16), the dynamic pressure, *R* in equation (5), and the total wetted surface area. The wetted surface area is computed by integrating the sum of the wetted linear elements at each station (as computed in the volume calculation) along the total wetted length of the hull. The wave making resistance is computed externally using CFD and is entered as a lookup table versus speed and draft. No corrections are made for the instantaneous position of each station due to waves but the overall draft and length due to current conditions are taken into account.

If the Froude number is between 1.1 and 1.2, a linear combination of the forces is taken dependant on the proximity of the Froude number to either condition. Equations (23) and (24) show the linear combination of the forces.

$$F_x = F_{x_{planing}}\left(1.2 - Fn\right) + F_{x_{displacement}}\left(Fn - 1.1\right) \tag{23}$$

$$F_z = F_{z_{planing}}\left(1.2 - Fn\right) + F_{z_{displacement}}\left(Fn - 1.1\right) \tag{24}$$

Here we see that $F_{x_{planing}}$ and $F_{z_{planing}}$ are the forces in *x* and *z* computed using equation (22) and equation (10) respectively. $F_{x_{displacement}}$ and $F_{z_{displacement}}$ are the forces in *x* and *z* computed using the frictional drag and the wave making drag, as computed in CFD, and the buoyancy as described above, respectively.

In select cases, the effects of aerodynamics on the hull are of interest. This force is only included in the simulation if the hull becomes airborne. In essence, this force is the resistance force of the hull free-falling after lifting from a wave. The force coefficients must be input as user-defined data (most likely calculated using CFD). If the aerodynamics model is used, a Dryden wind model (The MathWorks 2007) is present. The wind is assumed to be unidirectional, and the instantaneous angle between the hull and the developed sea spectrum is assumed to be the direction of the wind at the current station. The angle is then averaged over the entire hull length. The force is computed by assuming the hull is a blunt object in the wind field yielding a constant force coefficient. The frontal area is entered by the user.

2.3 Lifting Body Dynamics

As in the hull case, the addition of multiple lifting bodies is trivial. For that reason, all discussion here assumes a single lifting body.

The computation of the force on a lifting body is separated into three parts: the vertical force, the resistance, and the added mass/damping forces due to viscous effects. The vertical force has a buoyant component and a dynamic component. If the user chooses to input the force coefficients including the buoyant forces, the buoyancy is not computed automatically. Otherwise, the buoyancy is computed identically to the hull buoyancy. It is assumed, however, that the entire body is submerged at all times. This is not necessarily a good assumption in all cases, however, and changes will be made to the code to allow for partially or totally dry lifting bodies. The dynamic portion of the vertical force is found by interpolating a series of curve fits or surface fits. The typical variables are depth of submergence of the body (in this case, the body can be partially or totally dry), angle of attack of the body, which depends on water velocities as well as boat velocities (linear and angular), inflow velocity which again depends on the linear and angular velocities of the boat and water, and flap angles (if flaps are present).

The resistance forces are similarly computed by interpolating from a series of curve fits or surfaces from user-supplied data.

No checks are currently made for flow separation or cavitation on the lifting body. It is assumed that the force coefficients supplied by the user take into account all possible operating conditions.

If struts are included, the forces generated are currently computed internally by the simulation; there is no mechanism for user-input of force coefficients for struts. The strut forces are computed using lift and drag coefficients for a typical NACA section. The inflow velocity and angles are computed for a single point halfway between the free surface and the deepest part of the foil; see Figure 3. The wetted length is computed by averaging the wetted length of the leading edge and the trailing edge of the strut. The strut is considered uniform across its entire span.

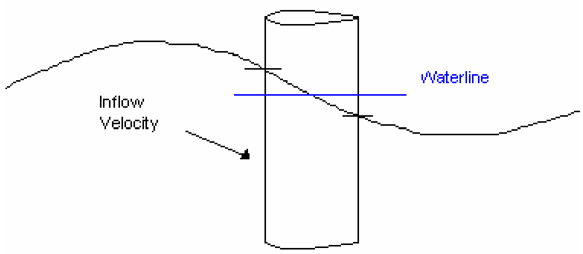

Figure 3: Computation of Strut Forces

The added mass of a lifting body is assumed to be a hemisphere of water of radius equal to the chord of the body. The viscous damping terms are a linear and a quadratic multiplier of the velocity of the body and the velocity of the body times its magnitude, respectively. The multipliers are user-defined inputs and are computed from model tests or full-scale tests of similar geometries.

2.4 Wave Spectra

The development of a realistic seaway is one of the main advantages of using a time-domain code over a frequency-based code. For this simulation, the user enters a significant wave height and period and specifies whether or not a distributed spectrum is desired (unidirectional is the default). The seaway is approximated using 50 waves in each direction with the number of directions entered by the user (the default is 21). In general, wave heights and velocities are only calculated where computationally necessary (points along the hull or body, for example). However, if the animation output option is used, the wave heights at a regular grid surrounding the boat must be computed increasing the total run time of the simulation.

The wave height and velocity at a given point are computed using the equations for a Pierson-Moskowitz spectrum (Lewis ed. 1988) as follows.

First we compute the encounter frequency at the i^{th} wave component (f_i) where the total spectrum is broken up into $\#wave$ components. Here ω_i is the frequency of the wave component, V is the forward velocity of the boat, θ is the angle between the direction of the waves and the direction of the boat, and g is the gravitational constant.

$$f_i = \omega_i \left(1 - \frac{\omega_i V \cos(\theta)}{g}\right) \tag{25}$$

Next we compute the wave height, h, due to the waves coming from a given direction, φ, by summing over all of the wave components in that direction. A_i is the wave component amplitude, N_i is the wave component wave number, ζ is the location in space where the wave height is being computed, ϕ_i is the phase shift of the wave component, and t is the current time in seconds.

$$h(\varphi) = \sum_{i=1}^{\#wave} A_i \sin\left(N_i \zeta + \phi_i + f_i t\right) \tag{26}$$

To compute the total wave height at the desired location, H, the components from equation (26) are summed over the number of directional slices and multiplied by the square of the cosine of the difference between the straight ahead direction and the given slice's direction. There is a constant required, shown in equation (27) as C, to ensure that the total energy in the wave spectrum is equal to the unidirectional case (US Army 1985).

$$H = \sum_{\#directions} h(\varphi) C \left[\cos(\varphi - \varphi_0)\right]^2 \tag{27}$$

The longitudinal (parallel to wave motion) and vertical (perpendicular to wave motion) velocity components for each direction are computed using equation (28) and equation (29) respectively.

$$u(\varphi) = \sum_{i=1}^{\#wave} A_i \omega_i e^{N_i H} \sin\left(N_i \zeta + \phi + f_i t\right) \quad (28)$$

$$w(\varphi) = \sum_{i=1}^{\#wave} -A_i \omega_i e^{N_i H} \cos\left(N_i \zeta + \phi + f_i t\right) \quad (29)$$

The total wave velocities are then computed in a similar manner as the total wave height was computed in equation (27); see equations (30) and (31).

$$U = \sum_{\#directions} u(\varphi) C\left[\cos\left(\varphi - \varphi_0\right)\right]^2 \quad (30)$$

$$W = \sum_{\#directions} w(\varphi) C\left[\cos\left(\varphi - \varphi_0\right)\right]^2 \quad (31)$$

2.5 Control System

The control system is simulated as an isolated section of user-specified code. The code can be either a block of MATLAB code or a dynamic link library containing appropriate links to the MATLAB environment. The simulation passes the state vector to the control system block and looks for the returned actuator positions. The simulation can thus be used to test compiled versions of control code before they are installed on a boat.

The simulation has a built-in high-fidelity model of our specific control computer and voter (the device that selects the signal to pass on to the actuator). The simulation also includes models of the servo system and all hydraulic parts moving the actuator. Thus the inner control loop can be accurately modeled, providing the user with a high-confidence prediction of system behavior rather than an idealized approximation of that behavior. The presence of the model of the inner control loop also gives the user the ability to design the system to properly control the actuators. Figure 4 shows a block diagram of the inner control loop model. The first expanded block in the diagram is the physical model of the actuation system. Within that, there is a block representing the servo dynamics and also a physical model (Ferreira et al. 2002) of the hydraulic cylinder valve (labeled as Kq), which is also expanded.

Because the update rate of the control computer is independent of the rest of the time simulation (especially if adaptive time stepping is used) care is taken to ensure that the time stepping is done correctly. Additionally, the time step required for temporal convergence of the actuation simulation is most likely different than that required for the boat simulation (typically, the actuation system is much stiffer than the boat). For this reason, care must be taken when choosing the correct time step for the overall system.

In addition to testing existing control systems on a given system, the simulation can also be used to assist in the designing of systems. The simulation can compute the linear state matrix and input matrix (A and B, respectively), as shown in equation (32), by perturbing the system in five directions (y, z, roll, pitch, yaw), as well as perturbing five velocities (sideslip, vertical velocity, roll velocity, pitch velocity, yaw velocity). This is accomplished at a series of speeds allowing the user to design a control system using these linearized systems across the entire speed range.

$$\dot{x} = Ax + Bu \quad (32)$$

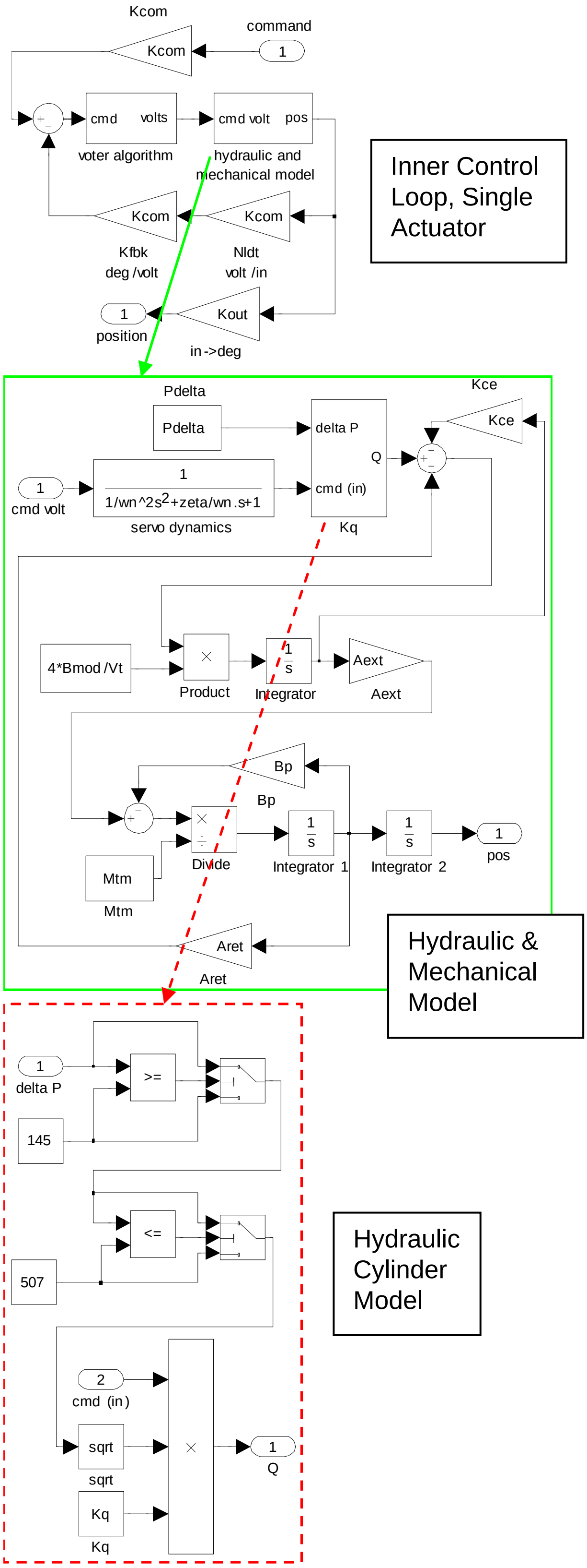

Figure 4: Block Diagram of Actuation Model

2.6 Other Features

It is often desirable to start the vessel from an equilibrium position without knowing this location a priori. The simulation includes a routine to compute the equilibrium position and place the vessel in that position if so desired. The equilibrium can be computed in one of two ways: the boat can be placed in a position that zeroes the forces and moments while holding the control surfaces fixed, or the control surfaces can be placed in positions that zero the forces and moments while holding the boat fixed. In both cases, the Newton-Raphson minimization for multiple variables (Press et al. 1988) is used. Equations (33) and (34) show the system of equations being minimized.

$$\sum F(\Phi,\Theta) = ma \tag{33}$$

$$\sum M(\Phi,\Theta) = I\omega \tag{34}$$

In these equations, Φ is the current state of the vehicle (positions and velocities), Θ is the state of the control surfaces (positions), m is the mass of the vehicle, I is the mass moment of inertia of the vehicle, a is the linear acceleration of the vehicle, ω is the angular acceleration of the vehicle, F is the total linear force, and M is the total moment.

For simplicity, in the control surface fixed case, the boat is only allowed to move in the z, roll, and pitch directions and all velocities are assumed fixed (forward velocity is held at some desired speed and sideslip velocity, vertical velocity, and all angular velocities are assumed zero). In the boat fixed case, all control surfaces are allowed to move. If the equilibrium position is found to be outside the allowable range of motion of the flaps or is unattainable, the simulation is stopped. Upon completion of the equilibrium placement, the required thrust for the given condition is reported.

The simulation also has a model of a ballasting system available. This lets the user simulate the effects of taking on or ejecting water underway and in a seaway. The ballasting system can be included as a part of the control system, allowing the user to have an actively-controlled ballast system. The ballast simulation has the added benefit of allowing the user to simulate the effects of different ballasting situations in a seaway. Also included, although not yet fully integrated, is an allowance for permeability which will give the user the ability to simulate damage conditions in a seaway.

It is often useful to be able to model failures in control systems. For this reason, the simulation has the ability to model failures in any of the electronic components of the modeled control computer or any of the hydraulic components of the modeled actuator. The following reactions can occur: the control surface becomes locked in its current location; the control surface becomes locked hard to one extreme or the other; or the control surface weathervanes with the incoming flow. By doing this, the user can evaluate the effects of a control surface failure. Also modeled, for our control system, is failure detection and mitigation. For example, if a failure is detected, a control surface can be set to lock in place until the system is reset.

The ability to model the linear state matrix of the system about a given point is also useful for control system design. For this reason, a linear force generator is included. This function inputs a number of speeds and then places the boat at the correct depth and trim using the equilibrium calculation described above. The linear force coefficients for the boat are then computed about this point. A series of matrices at each speed are returned.

2.7 Output Format

The results of the simulation are output in three ways: an Excel spreadsheet, a binary data file, and an AVI video file. A new Excel spreadsheet is created every 15,000 time steps to prevent file sizes from becoming too large.

The AVI video file generation can be accomplished in two ways. First, the file can be generated as the simulation progresses. This can be slow as a depiction of the free surface must be created at every time step. Second, the video file can be generated after the simulation has completed. In this case, the binary data file is loaded and the movie is generated after the fact, allowing the user to analyze the data while the animation is generated. Figure 5 shows a still image from a simulation animation.

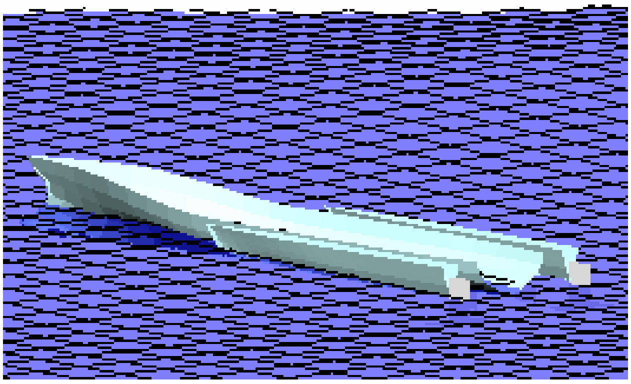

Figure 5: Still Image from Simulation Animation

3 COMPARISON WITH AT-SEA TEST DATA

A 21.3 m stabilized monohull with a bow lifting body and two aft T-foils was simulated. This boat is represented in Figure 1 and Figure 5. The linear force generator was used to design the control system. All inner loop control systems were also designed using the simulation. The boat was built and the control system is currently installed and operational on the vessel. Figure 6 shows the results of a simulation for head seas and 26 knots for in seas of 1.34 m significant height and significant period of 8.4 s. The simulation took approximately 0.36 seconds per time step (0.05 s), resulting in a total run time of approximately 42 minutes for the 5.8 minutes shown in the plot. Figure 7 shows corresponding data from at-sea tests of the boat for approximately the same conditions. Shown are the speed, bow height, and pitch. Comparing the two figures shows remarkable agreement between the simulation and the at-sea measurements.

Table 1 shows a comparison of statistical data for the time series data from the simulation and the at-sea test, from which it can be seen that the simulation correlates well quantitatively. The flap motions are very similar to the flap motions on the actual boat for similarly-sized waves. The forward flaps are moving slightly more on the as-tested boat, suggesting the sea state encountered in the real test was slightly larger than the one simulated.

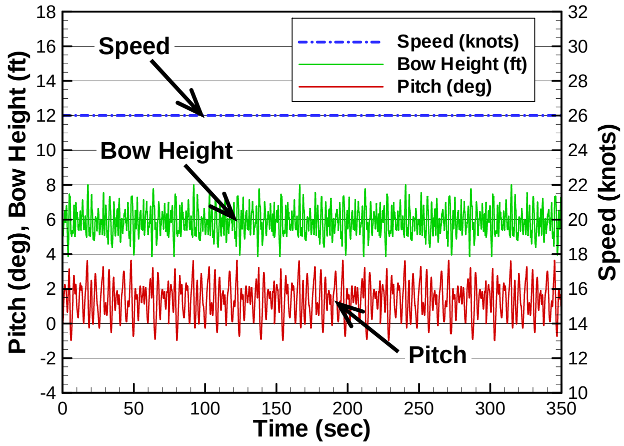

Figure 6: Simulated Data for BLB-70: Head Seas, 26 knots

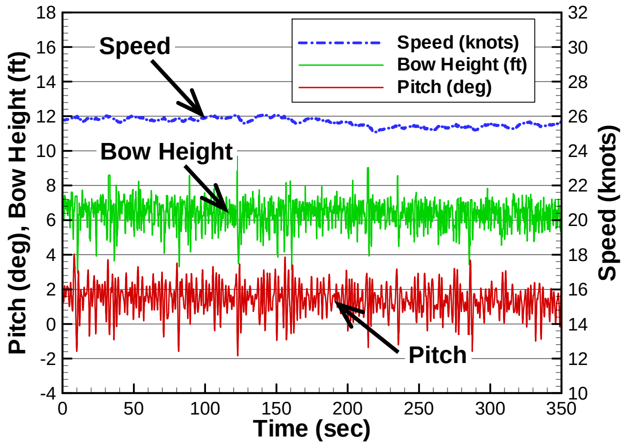

Figure 7: Actual Data for BLB-70: Head Seas, 26 knots

Table 1: Comparison of Statistical Data for BLB70 in Sea State 3 Head Seas

	Simulated		**As Tested**	
	RMS Values	Ave. Values	RMS Values	Ave. Values
Pitch (*deg*)	0.965	1.380	0.729	1.005
Bow Height (*ft*)	0.745	5.885	0.776	6.316
Fwd Flaps (*deg*)	0.258	0.125	1.577	1.093
Aft T-Foils (*deg*)	2.405	5.185	2.314	5.058
Vert. Accel. (*g*)	0.126	—	0.143	—

5 CONCLUSIONS

We have successfully developed a fast nonlinear simulation that can provide a reasonably accurate time-domain seakeeping simulation of a general class of ships of arbitrary geometry, which can incorporate lifting bodies and/or hydrofoils. This medium-fidelity solution offers the following advantages.

- The simulation allows the user to easily check changes to control system parameters in both the inner and outer control loops.
- Working in the time-domain allows the user to directly visualize the simulated system via AVI file.
- By using a combination of CFD data, semi-empirical formulae, and first principles equations, an accurate representation of the boat has been developed that is computationally efficient.
- By keeping the control system as an external block of code, alternative versions of control system code, including the actual as-installed version, can be tested.
- Accuracy in modeling of the actuation system components allows the designer to create a failure detection and mitigation system with confidence.

Comparison of data from the simulation with at-sea test data shows excellent correlation, giving further confidence in the simulation's validity as an analysis tool to aid in control system design.

ACKNOWLEDGEMENTS

Much of the work described in this paper has been made possible with support from the Office of Naval Research.

REFERENCES

Ambardar, A. (1995). Analog and Digital Signal Processing. PWS Publishing Company.

Beck, R. & Reed, A. (2000). 'Modern Seakeeping Computations for Ships.' Proceedings of the 23rd Symposium on Naval Hydrodynamics. Val de Reuil, France.

Breslin, J. P. (2001). 'Chines-Dry Planing of Slender Hulls: A General Theory Applied to Prismatic Surfaces.' Journal of Ship Research **45**(1) pp. 59-72.

Ferreira, J. A., Gomes de Almeida, F. & Quintas, M. R. (2002). 'Semi-empirical model for a hydraulic servo-solenoid valve.' Proceedings of the Institution of Mechanical Engineers, Part I, Journal of Systems and Control Engineering **216**(3) pp.237-248.

Lewis, E. V. (ed.). (1988). Principles of Naval Architecture. The Society of Naval Architects and Marine Engineers.

Piegl, L. A. & Tiller, W. (1997). The NURBS Book. 2nd ed. Springer-Verlag, New York.

Press, W. H et al. (1988). Numerical Recipes in C. Cambridge University Press.

The MathWorks, Inc. (2007). 'Dryden wind turbulence model (continuous).' <http://www.mathworks.ch/products/aeroblks/blocklist.html>.

US Army Engineer Waterways Experiment Station, Coastal Engineering Research Center. (1985) 'Directional Wave Spectra Using Cosine Squared and Cosine 2S Spreading Functions.' CETN-I-28. Vicksburg, Miss.